Graded Projected Entangled-Pair State Representations and An Algorithm for Translationally Invariant Strongly Correlated Electronic Systems on Infinite-Size Lattices in Two Spatial Dimensions

Qian-Qian Shi,[1] Sheng-Hao Li,[1] Jian-Hui Zhao,[1] and Huan-Qiang Zhou[1]

[1]*Centre for Modern Physics and Department of Physics,*
Chongqing University, Chongqing 400044, The People's Republic of China

An algorithm to find a graded Projected Entangled-Pair State representation of the ground state wave functions is developed for translationally invariant strongly correlated electronic systems on infinite-size lattices in two spatial dimensions. It is tested for the two-dimensional $t - J$ model at and away from half filling, with truncation dimensions up to 6. We are able to locate a line of phase separation, which qualitatively agrees with the results based on the high-temperature expansions. We find that the model exhibits an extended s-wave superconductivity for $J = 0.4t$ at quarter filling. However, we emphasize that the currently accessible truncation dimensions are not large enough, so it is necessary to incorporate the symmetry of the system into the algorithm, in order to achieve results with higher precision.

The investigation of models of strongly correlated electrons in two spatial dimensions remains to be a major challenging issue in condensed matter physics. Actually, no well-controlled analytical techniques are available to study even the ground state properties, which has led numerous theorists to appeal to numerical simulations. Up to now, some powerful numerical approaches to classically simulate quantum many-body lattice systems have been proposed, such as Quantum Monte Carlo (QMC) [1] and the Density Matrix Renormalization Group (DMRG) [2]. However, the QMC suffers from a notorious sign problem for both strongly correlated electronic systems and frustrated spin systems, whereas the DMRG is not so efficient for quantum lattice many-body systems in two spatial dimensions.

Recently, significant advances have been made in the context of classical simulations of quantum lattice many-body systems in terms of the so-called Tensor Network (TN) algorithms [3, 4, 5, 6, 7, 8, 9, 10]. These include the Matrix Product States (MPS) [11] for quantum lattice systems in one spatial dimension, the Projected Entangled-Pair States (PEPS) [6] for quantum lattice systems in two and higher spatial dimensions, and the Multi-scale Entanglement Renormalization Ansatz (MERA) [10] for quantum lattice systems in any spatial dimensions. One of the advantages of the TN algorithms is that, in contrast to the QMC, they do not suffer from any sign problem, although a graded version of the TN algorithms is necessary to take into account all signs arising from the anti-commutivity of fermionic operators at different lattice sites. Therefore, it is highly desirable to develop efficient graded TN algorithms that enable us to classically simulate quantum electronic lattice systems in two spatial dimensions. Remarkably, algorithms to tackle signs arising from the anti-commutivity of fermionic operators at different lattice sites for strongly correlated electronic systems have recently been proposed in the context of the MERA representations [12].

In this paper, we develop a numerical algorithm to find a graded Projected Entangled-Pair State (gPEPS) representation of the ground state wave functions for translationally invariant strongly correlated electronic systems on infinite-size lattices in two spatial dimensions. In our opinion, the gPEPS is a natural extension of the PEPS to tackle quantum electronic lattice systems, in which a parity is attached to each of the basis vectors of both auxiliary and physical spaces that are super spaces in mathematics. The algorithm is tested for the two-dimensional $t - J$ model at and away from half filling, with truncation dimensions up to 6. We are able to locate a line of phase separation (PS), which qualitatively agrees with the results based on the high-temperature expansions [13]. We find that the model exhibits an extended s-wave superconductivity for $J = 0.4t$ at quarter filling. However, we emphasize that the currently accessible truncation dimensions are not large enough, so it is necessary to incorporate the symmetry of the system into the algorithm, in order to achieve results with higher precision.

Graded PEPS representations. Consider a translationally invariant quantum electronic system on an infinite-size square lattice in two spatial dimensions. Suppose it consists of the nearest-neighbor interactions, characterized by a Hamiltonian $H = \sum_{<ij>} h_{<ij>}$. Our purpose is to find the ground state wave function via an imaginary time evolution, with a randomly chosen state as an initial state $|\psi_0\rangle$:

$$|\psi_\tau\rangle = \frac{\exp(-H\tau)|\psi_0\rangle}{\|\exp(-H\tau)|\psi_0\rangle\|}, \qquad (1)$$

when $\tau \to \infty$, as long as the initial state is not orthogonal to the genuine ground state.

In order to carry out the imaginary time evolution efficiently, we need to represent the system's ground state wave functions in terms of graded PEPS states for translationally invariant strongly correlated electron systems on infinite-size square lattices in two spatial dimensions. At each site, there is a local d-dimensional Hilbert super space V whose basis vectors are $|s\rangle$ ($s = 1, 2, \cdots, d$), with the parity $[s]$ being 0 for even vectors and 1 for odd vectors. In the graded version of the valence bond state (gVBS) picture [14], one may associate four $\mathbb{D}$-dimensional auxiliary super spaces V_l, V_r, V_u,

and V_d to the physical Hilbert super space V. Suppose $|l\rangle$, $|r\rangle$, $|u\rangle$, and $|d\rangle$ are bases of the auxiliary super spaces V_l, V_r, V_u, and V_d, with their corresponding parities $[l]$, $[r]$, $[u]$ and $[d]$, respectively. Following Ref. [6], we define a gVBS state

$$|\Psi\rangle = \prod_{h,v} P_{h,v} \otimes |\phi\rangle, \qquad (2)$$

where $|\phi\rangle$ is a maximally entangled state $|\phi\rangle = \sum_{n=1}^{\mathbb{D}} |n, n\rangle$, the tensor product $\otimes$ is over all possible bonds on the square lattice, and P is a projection operator $P: V_l \otimes V_r \otimes V_u \otimes V_d \rightarrow V$, defined as

$$P = \sum_{l,y,u,d=1}^{\mathbb{D}} \sum_{s=1}^{\mathrm{d}} W_{lrud}^s |s\rangle\langle lrud|. \qquad (3)$$

For convenience, we assume that $W_{lrud}^s = 0$ if $[s] + [l] + [r] + [u] + [d] \neq 0 \bmod 2$. Substituting Eq. (3) into Eq.(2), and taking into account the signs arising from the grading structure, under the convention that physical states $|s\rangle$ on a square lattice are arranged by first ordering from left to right along horizontal bonds and then from up to down along vertical bonds, we may map a gVBS to a gPEPS described by a seven-index tensor $\tilde{W}_{lrud;l'r'}^s$:

$$W_{lrud;l'r'}^s = (-1)^{[r]([u]+[d])} (-1)^{dr'} W_{lrud}^s \, \delta_{l'+r'+[u]+[d] \bmod 2, \, 0}. \quad (4)$$

Here, l' and r' ($l', r' = 0, 1$) are indices labeling two extra horizontal grading bonds attached to each lattice site (see Fig. 1(i)). The gPEPS for this convention is visualized in Fig. 1(ii). However, there exists another equivalent representation

$$W_{lrud;l'r'}^s = (-1)^{[r]([u]+[d])} (-1)^{ul'} W_{lrud}^s \, \delta_{l'+r'+[u]+[d] \bmod 2, \, 0}. \quad (5)$$

We emphasize that, as we shall see later on, this convention is *only* useful to absorb a two-site gate acting on a horizontal bond during the imaginary time evolution. In order to absorb a two-site gate acting on a horizontal bond during the imaginary time evolution, we need another convention that physical states $|s\rangle$ on a square lattice are arranged by first ordering from up to down along horizontal bonds and then from left to right along vertical bonds, which yields other two equivalent representations:

$$W_{udlr;u'd'}^s = (-1)^{[d]([l]+[r])} (-1)^{rd'} W_{udlr}^s \, \delta_{u'+d'+[l]+[r] \bmod 2, \, 0}, \quad (6)$$

and

$$W_{udlr;u'd'}^s = (-1)^{[d]([l]+[r])} (-1)^{lu'} W_{udlr}^s \, \delta_{u'+d'+[l]+[r] \bmod 2, \, 0}. \quad (7)$$

Here, u' and d' ($u', d' = 0, 1$) are indices labeling two extra vertical grading bonds attached to each lattice site, as shown in Fig. 1(iv). Note that W_{udlr}^s is related to W_{lrud}^s via $W_{udlr}^s = (-1)^{([l]+[r])([u]+[d])} W_{lrud}^s$. The gPEPS for this convention is visualized in Fig. 1(v).

Note that Eq. (4) has been introduced in Ref. [15] in the context of a fermionic PEPS (fPEPS) representation. However, an essential difference between an fPEPS and a gPEPS

lies in the fact that the latter may be used to absorb a two-site gate during the imaginary time evolution which acts on a horizontal bond or vertical bond (see below). In addition, it is convenient to use super spaces that naturally describe physical Hilbert spaces in the two-dimensional $t - J$ model.

The algorithm. As usual, the imaginary time evolution operator $\exp(-H\tau)$ in Eq. (1) is implemented by dividing τ into M small time slices $\delta\tau$: $\tau = M\delta\tau$. For each small time slice $\delta\tau$, it is represented by $\exp(-H\delta\tau)$. In fact, for our purpose, we shall choose a plaquette as a unit cell, with its vertices labeled as W, X, Y and Z (see Fig. 1(iii) and Fig. 1(vi)). Then, as follows from the Suzuki-Trotter decomposition [16], $\exp(-H\delta\tau)$ is a product of eight different kinds of two-site gates U_α ($\alpha = WX, XW \, YZ, ZY \, WY, YW, XZ, ZX$) corresponding to eight different kinds of bonds, with the two-site gate U_α defined by

$$U_\alpha \equiv \exp(-h_\alpha \delta\tau), \quad \delta\tau \ll 1. \qquad (8)$$

Thus, we have reduced the problem to implement the imaginary time evolution to how to update the gPEPS tensors W, X, Y, and Z under the action of a two-site gate U_α acting on eight different types of bonds. An efficient (but not optimal) way to do this is to adapt the strategy used in the iMPS algorithm [7]. Therefore, we attach a diagonal singular value matrix λ_α to each type of bonds, with tensors Γ_W, Γ_X, Γ_Y, and Γ_Z defined via removing a square root of the singular value matrix from each of all four bonds surrounding W, X, Y, and Z, respectively. As such, the algorithm consists of two parts: first, absorb the action of a two-site gate U_α on a gPEPS to update the gPEPS tensors; second, read out the expectation value of a physical observable in a given gPEPS.

(i) *Updating of the gPEPS tensors.* Our choice of the unit cell in the gPEPS representation assumes that it is translationally invariant under two-site shifts, which implies that one only needs to address two consecutive sites linked by a certain kind of bonds; once this is done, we simultaneously update all the tensors on the sites linked by the same kind of bonds. The updating procedure for a two-site gate acting on a WX bond is visualized in Fig. 2, which consists of a few steps: (i) the two-site gate U_α is applied onto the gPEPS. (ii) A single tensor Θ is formed by contracting the tensors Γ_W, Γ_X, λ_{xw}, λ_{zx}, λ_{xz}, λ_{wy}, λ_{yw}, and the gate U_α. (iii) Reshape the tensor Θ into a matrix M. (iv) A singular value decomposition (SVD) is performed for the matrix M, followed by a truncation, with only the $\mathbb{D}$ largest singular values retained in the updated singular matrix λ'_{wx}. (v) Reshape the matrices U and V into the tensors $\tilde{U}$ and $\tilde{V}$. (vi) Recover the diagonal matrix λ_{xw}, λ_{zx}, λ_{xz}, λ_{wy}, λ_{yw}, and update the tensors Γ_W and Γ_X to be Γ'_W and Γ'_X.

(ii) *Measuring a physical observable.* Once a gPEPS is generated as a ground state wave function of a translationally invariant quantum electronic system on an infinite-size square lattice, we need to compute the expectation value of a physical observable. For this purpose, the basic building blocks are double tensors w, x, y and z formed from contracting the physical indices for the gPEPS tensors W, X, Y, and Z and
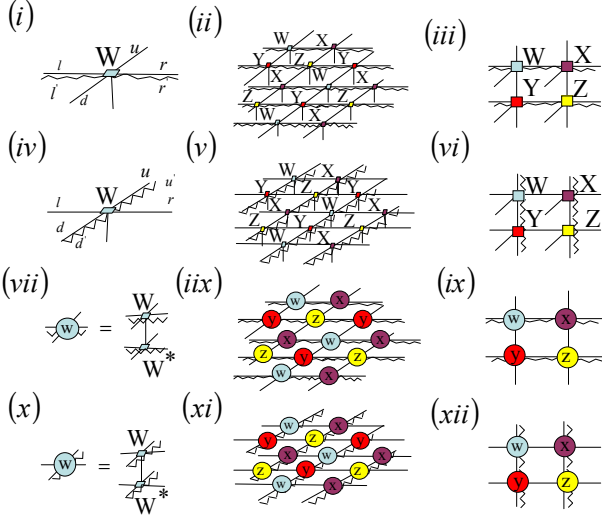
FIG. 1: (color online) (i) and (iv): Seven-index tensors, $W^s_{ludr;l'r'}$ and $W^s_{ulrd;u'd'}$ used to represent a gPEPS representation of the system's ground state wave functions for an infinite-size system, with s being a physical index, l, r, u, and d denoting the inner indices. Here, l', r', u' and d' are horizontal and vertical grading indices, respectively. (ii) and (v): The pictorial representation of a gPEPS $|\psi\rangle$ with horizontal and vertical grading bonds, which are used to absorb a two-site gate acting on horizontal and vertical bonds, respectively. (iii) and (vi): The unit cells of an infinite gPEPS with horizontal and vertical grading bonds, respectively, made of four seven-index tensors W, X, Y, and Z. (vii) and (x): Double tensors $w_{ludr;l'r'}$ and $w_{ulrd;u'd'}$ are formed from the seven-index tensors W and theirs complex conjugates W^* with horizontal and vertical grading bonds, respectively. (viii) and (xi): The tensor networks (TNs) for the norm of gPEPS's with horizontal and vertical grading bonds, respectively. (ix) and (xii): The unit cells of the TNs for the norm of gPEPS's with horizontal and vertical grading bonds, respectively.

their complex conjugates (see Fig. 1(vii) and Fig. 1(x)), respectively. As such, one may visualize the norm for a gPEPS as a TN, as shown in Fig. 1(viii) and Fig. 1(xi), with their unit cells plotted in Fig. 1(ix) and Fig. 1(xii). With the double tensors w, x, y and z as the building blocks, one may form the one-dimensional transfer matrix E_1, which is a Matrix Product Operator on an infinite strip (see Fig. 3). The left and right eigenvectors corresponding to the largest eigenvalue of E_1 are iMPS's, from which one may form the zero-dimensional transfer matrix E_0 (see Fig. 4(i)). The largest left and right eigenvectors of E_0 are defined in Fig. 4(ii), which, together with those of E_1, form the environment tensors. In addition, an auxiliary vector V'_R is defined by absorbing the tensors Σ_3, Σ_4, Σ'_2, Σ'_3, y, and z, as visualized in Fig. 4(iii). This enables us to compute the ground state energy for the XW bond, as shown in Fig. 4(iv).

The same procedure may be used to update the gPEPS tensors and to read out a physical observable for other bonds. However, different conventions should be adopted for horizontal and vertical bonds.

We stress that the update procedure above is *not* optimal, in the sense that it does not produce the best approximate
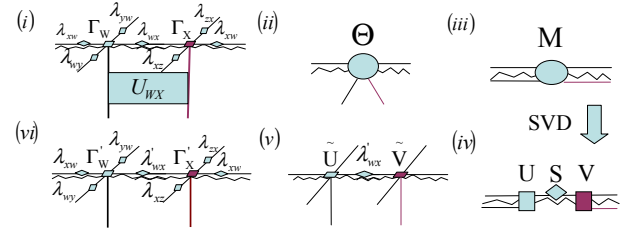

FIG. 2: (color online) The procedure to update the gPEPS tensors Γ_W and Γ_X and the singular value matrix λ_{wx} via absorbing the action of a two-site gate U_α. (i) the two-site gate U_α is applied onto the gPEPS. (ii) A single tensor Θ is formed by contracting the tensors Γ_W, Γ_X, λ_{xw}, λ_{zx}, λ_{xz}, λ_{wy}, λ_{yw}, and the gate U_α. (iii) Reshape the tensor Θ into a matrix M. (iv) A singular value decomposition (SVD) is performed for the matrix M, followed by a truncation, with only the $\mathbb{D}$ largest singular values retained in the updated singular matrix λ'_{wx}. (v) Reshape the matrices U and V into the tensors $\tilde{U}$ and $\tilde{V}$. (vi) Recover the diagonal matrix λ_{xw}, λ_{zx}, λ_{xz}, λ_{wy}, λ_{yw}, and update the tensors Γ_W and Γ_X to be Γ'_W and Γ'_X.
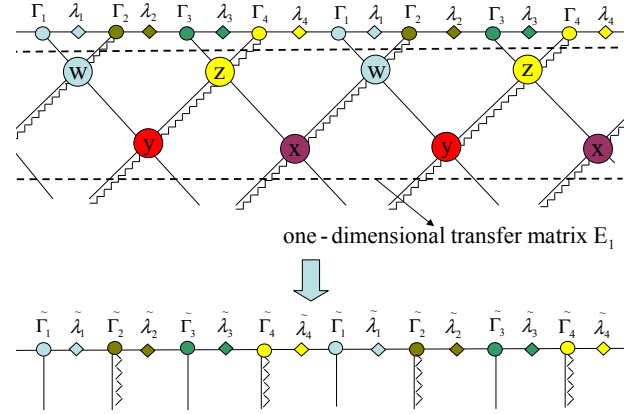

FIG. 3: (color online) The iMPS used to approximate the largest eigenvector of the one-dimensional transfer matrix E_1, shown here as an Matrix Product Operator on an infinite strip. Here, we need to absorb two-site nonunitary gate acting on an iMPS. The iMPS turns out to be the largest eigenvector of the transfer matrix E_1 if λ_1, λ_2, λ_3, and λ_4 converge after the transfer matrix E_1 is acted on the iMPS enough times.

gPEPS representation for each imaginary time slice during the imaginary time evolution. As such, our update procedure can *only* be used to produce the system's ground state wave functions, but *not* for real time evolution from a prescribed initial state. A similar situation occurs for an MPS algorithm [9]. This drawback may be remedied if one uses the same strategy as the iPEPS algorithm [17], which is *optimal* in the above sense. That is, in order to absorb a two-site gate, one needs to compute the environment tensors, i.e., the left and right largest eigenvectors of both the one-dimensional and zero-dimensional transfer matrices for each time slices. Therefore, the update problem is reduced to a four-site sweep procedure that consists of successively solving a set of linear equations [4]. However, this requires to update the environment tensors as we update the gPEPS tensors W, X, Y, and Z for each two-site gate, so it is much less efficient.
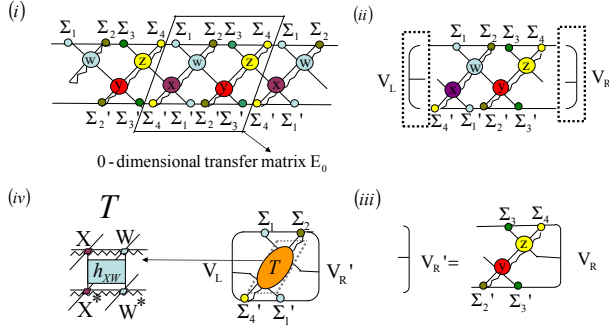
FIG. 4: (color online) The ground state energy per bond is computed by contracting the environment tensors, with the XW bond as an example. (i) The right and left largest eigenvectors of the transfer matrix E_1 are denoted by tensors Σ_1, Σ_2, Σ_3, Σ_4, and Σ'_1, Σ'_2, Σ'_3, Σ'_4, respectively. Here, the 0-dimensional transfer matrix E_0 is visualized. (ii) The largest left and right eigenvectors V_L and V_R of the one-dimensional transfer matrix E_0. (iii) An auxiliary vector V'_R is defined by absorbing the tensors Σ_3, Σ_4, Σ'_2, Σ'_3, y, and z. (iv) The ground state energy for the XW bond is computed by contracting a tensor T with the tensors V_L, V'_R, Σ_1, Σ_2, Σ'_1, and Σ'_4. Here, T is defined by the Hamiltonian density h_{XW} and the tensors x, w, x^*, and w^*.
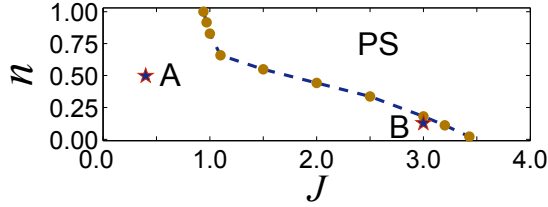

FIG. 5: (color online) For $J \geq 0.95$, there is a line of phase separation (PS). For $J \leq 0.95$, no PS occurs. Here, we have chosen $\mathbb{D} = 4$. For $J = 0.4$ and $n = 0.4968$, denoted as A, the extended s-wave pairing order parameter $<\Delta> = 0.083 + 0.11i$, with the ground state energy per site $e = -0.9498$ for $\mathbb{D} = 6$. For $J = 3.0$ and $n = 0.1273$, denoted as B, the extended s-wave pairing order parameter $<\Delta> = 0.010 + 0.055i$, with the ground state energy per site $e = -0.4157$ for $\mathbb{D} = 4$.

Simulation of the two-dimensional $t - J$ model. We test the algorithm with the two-dimensional $t - J$ model described by the Hamiltonian [18]:

$$H = -t \sum_{<ij>\sigma} [\mathcal{P}(c^\dagger_{i\sigma}c_{j\sigma} + \text{H.c.})\mathcal{P}] + J \sum_{<ij>} (\mathbf{S}_i \cdot \mathbf{S}_j - \frac{1}{4}n_i \, n_j), \quad (9)$$

where $\mathbf{S}_i$ are spin $1/2$ operators at a lattice site i, $\mathcal{P}$ is the projection operator excluding double occupancy, and t and J are, respectively, the hoping constant and anti-ferromagnetic coupling between the nearest neighbor sites $<ij>$. Hereafter, we shall choose $t = 1$ for brevity.

At half filling (i.e., $n = 1$, with n being the number of electrons per site), the $t - J$ model reduces to the two-dimensional Heisenberg model. In this case, the algorithm yields the ground state energy per site $e = -1.1675J$, for the truncation dimension $\mathbb{D} = 4$, quite close to the QMC simulation result $e = -1.1680J$ [19, 20]. Away from half filling, the model exhibits different behaviors for small and large antiferromagnetic coupling J, see Fig. 5. For $J \geq 0.95$, there is a line of PS. For $J \leq 0.95$, no PS occurs. This agrees qualitatively with the results based on the high-temperature expansions [13]. Note that our result for the transition point $J_c = 3.43$ at low electron density is quite close to the exact value $J_c = 3.4367$ [21]. Here, we have chosen $\mathbb{D} = 4$.

In the homogeneous regime, it turns out that the algorithm does not yield much conclusive results, due to the fact that the truncation dimension $\mathbb{D}$ currently accessible is quite small (up to $\mathbb{D} = 6$). However, signals of extended s-wave superconductivity are observed in two regimes: the first is the regime for $2 < J < 3.43$ at low electron density, and the second is the regime which starts at least from $J = 0.4$ at (almost) quarter filling. For $J = 0.4$ and $n = 0.4968$, denoted as A in Fig. 5, the extended s-wave pairing order parameter $<\Delta> = 0.083 + 0.11i$, with the ground state energy per site $e = -0.9498$ for $\mathbb{D} = 6$. For $J = 3.0$ and $n = 0.1273$, denoted as B in Fig. 5, the extended s-wave pairing order parameter $<\Delta> = 0.010 + 0.055i$, with the ground state energy per site $e = -0.4157$ for $\mathbb{D} = 4$. It remains unclear whether or not these two points are continuously connected.

Given that the bottleneck of the algorithm to achieve higher precision is the smallness of the truncation dimension $\mathbb{D}$, we expect that our data may be significantly improved for a larger truncation dimension $\mathbb{D}$ by incorporating the symmetry into the algorithm [22]. Indeed, even for the anti-ferromagnetic order parameter at half filling, the currently accessible truncation dimensions are still too small.

Summary and outlook. We have developed a numerical algorithm to find a gPEPS representation of the ground state wave functions for translationally invariant strongly correlated electronic systems on infinite-size lattices in two spatial dimensions. It is tested for the two-dimensional $t - J$ model at and away from half filling, with truncation dimensions up to 6. We are able to locate a line of PS, which qualitatively agrees with the results based on the high-temperature expansions [13]. It is proper to stress that the location of the line may vary if the truncation dimension is increased, although the variation might be small (especially at low electron density), due to the fact that PS can be seen from a consideration based on energetics [23], whereas the ground state energy per site we computed is reasonable, compared to the exact values for a small (4×4) cluster. In addition, the model exhibits an extended s-wave superconductivity for $J = 0.4t$ at quarter filling. However, we emphasize that the currently accessible truncation dimensions are not large enough, so it is necessary to incorporate the symmetry of the system into the algorithm, in order to achieve results with higher precision. This is currently under investigation.

After this work was completed, we have become aware of a preprint by T. Barthel, C. Pineda, and J. Eisert, arXiv:0907.3689, in which an alternative contraction scheme for the fermionic PEPS is discussed in the context of fermionic operator circuits. This work is supported in part

———

[1] D.M. Ceperley and B.J. Alder, Phys. Rev. Lett. **45**, 566 (1980).

[2] S.R. White, Phys. Rev. Lett. **69**, 2863 (1992); Phys. Rev. B **48**, 10345 (1993); U. Schollwoeck, Rev. Mod. Phys. **77**, 259 (2005).

[3] G. Vidal, Phys. Rev. Lett. **91**, 147902 (2003); Phys. Rev. Lett. **93**, 040502 (2004).

[4] F. Verstraete, D. Porras, and J.I. Cirac, Phys. Rev. Lett. **93**, 227205 (2004).

[5] H. Takasaki, T. Hikihara, and T. Nishino, J. Phys. Soc. Jpn. **68**, 1537 (1999).

[6] F. Verstraete and J.I. Cirac, cond-mat/0407066; V. Murg, F. Verstraete, and J.I. Cirac, Phys. Rev. A **75**, 033605 (2007).

[7] G. Vidal, Phys. Rev. Lett. **98**, 070201 (2007); R. Orús and G. Vidal, arXiv:0711.3960.

[8] H.-C. Jiang, Z.-Y. Weng, and T. Xiang, Phys. Rev. Lett. **101**, 090603 (2008); Z.-C. Gu, M. Levin, and X.-G. Wen, Phys. Rev. B **78**, 205116 (2008).

[9] Q.-Q. Shi and H.-Q. Zhou, J. Phys. A: Math. Theor. **42**, 272002 (2009).

[10] G. Vidal, Phys. Rev. Lett. **99**, 220405 (2007); Phys. Rev. Lett. **101**, 110501 (2008).

[11] M. Fannes, B. Nachtergaele, and R. Werner, Commun. Math. Phys. **144**,443 (1992); S. Östlund and S. Rommer, Phys. Rev. Lett. **75**, 3537 (1995).

[12] P. Corboz, G. Evenbly, F. Verstraete, and G. Vidal, arXiv:0904.4151; P. Corboz and G. Vidal, arXiv:0907.3184; C. Pineda, T. Barthel, and J. Eisert, arXiv:0905.0669; T. Barthel, C. Pineda, and J. Eisert, arXiv:0907.3689.

[13] W.O. Putikka, M.U. Luchini, and T.M. Rice, Phys. Rev. Lett. **68**, 538 (1992); E. Dagotto, J. Riera, Y.C. Chen, A. Moreo, A. Nazarenko, F. Alcaraz, and F. Ortolani, Phys. Rev. B **49**, 3548 (1994).

[14] F. Verstraete and J.I. Cirac, Phys. Rev. A **70**, 060302(R) (2004).

[15] C.V. Kraus, N. Schuch, F. Verstraete, and J. I. Cirac, arXiv:0904.4667.

[16] M. Suzuki, Phys. Lett. A **146**, 319 (1990); J. Math Phys. **32**, 400 (1991).

[17] J. Jordan, R. Orus, G. Vidal, F. Verstraete, and J. I. Cirac, Phys. Rev. Lett. **101**, 250602 (2008).

[18] For a review, see, e.g., E. Dagotto, Rev. Mod. Phys. **66**, 763 (1994) and references therein.

[19] For a review, see, E. Manousakis, Rev. Mod. Phys. **66**, 763 (1994) and references therein.

[20] D.A. Huse, Phys. Rev. B **37**, 2380 (1988); K.J. Runge, Phys. Rev. B **45**, 12292 (1992).

[21] C.S. Hellberg and E. Manousakis, Phys. Rev. B **52**, 4639 (1995).

[22] S. Singh, H.-Q. Zhou, and G. Vidal, arXiv:cond-mat/0701427; S. Singh, R.N.C. Pfeifer, and G. Vidal, arXiv:0907.2994.

[23] V.J. Emery, S.A. Kivelson, and H.Q. Lin, Phys. Rev. Lett. **64**, 475 (1990).